Available online at www.sciencedirect.com
SCIENCE DIRECT®
Chemical Physics Letters 390 (2004) 1–7
CHEMICAL PHYSICS LETTERS
www.elsevier.com/locate/cplett

A robust pulse sequence for the determination of small homonuclear dipolar couplings in magic-angle spinning NMR

Per Eugen Kristiansen [a], Marina Carravetta [b], Wai Cheu Lai [b], Malcolm H. Levitt [b,*]

[a] Department of Biochemistry, University of Oslo, P.O. Box 1041-Blindern, 0316 Oslo, Norway
[b] Department of Chemistry, School of Chemistry, Southampton University, Southampton SO17 1BJ, UK

Received 11 January 2004; in final form 17 March 2004
Available online 27 April 2004

Abstract

We present a new solid-state NMR pulse sequence that accomplishes efficient broad-band dipolar recoupling in systems with small dipolar couplings and large chemical shift anisotropies. The method involves a supercycled symmetry-based recoupling sequence incorporated in a constant-interval data acquisition strategy. The supercycle removes destructive higher-order average Hamiltonian terms, and makes the method more robust at long time intervals. We demonstrate 38.4% double-quantum filtering efficiency on diammonium [1,4-$^{13}C_2$]-fumarate in which the internuclear distance, as estimated by X-ray diffraction, is 387.8 pm. The estimated ^{13}C–^{13}C dipolar coupling was -136.5 ± 5.1 Hz, corresponding to an internuclear distance of 382.5 ± 4 pm.

1. Introduction

Solid-state nuclear magnetic resonance (NMR) is an increasingly powerful method for addressing molecular structural problems [1–20]. An important factor has been the combination of magic-angle spinning (MAS) and the development of accurate methods for internuclear distance determination. Dipolar recoupling methods such as rotational resonance [2], REDOR [3], DRAMA [4], HORROR [10], DRAWS [5–9] and the symmetry-based pulse sequences [11–20], have lead to a range of tools for internuclear distance determination with many applications in structural chemistry and biology.

The symmetry-based approach to pulse sequence design [11–20], allows the prediction of important features of the recoupling sequence, such as its orientation dependence and decoupling properties, on the basis of simple integer inequalities. In the context of homonuclear recoupling, sequences such as C7 [11], Post-C7 [12] and $R14_2^6$ [14] provide high double-quantum signal filtering efficiency, and make it possible to determine ^{13}C–^{13}C distances with picometer accuracy [15]. These sequences have the property of γ-encoding, which implies that to first-order, the recoupled double-quantum Hamiltonian is purely phase modulated by the third Euler angle describing the orientation of the molecules with respect to the rotating sample holder. γ-Encoding leads to high double-quantum filtering efficiencies and large dipolar oscillations for powder samples [10,11]. This allows the accurate determination of ^{13}C–^{13}C bond lengths even when the NMR signal is weak.

However, γ-encoded double-quantum recoupling sequences have not proven so suitable for the determination of longer distances between nuclei with relatively large chemical shift anisotropies, although attempts have been made [15]. Karlsson et al. [9] showed that non-γ-encoded sequences such as DRAWS [5–9] are generally superior for long range distance estimations, despite their lower theoretical efficiency in the absence of relaxation.

DRAWS is not based on symmetry principles and suffers from relatively inefficient local averaging of CSA interactions. In this Letter, we attempt to combine the favorable features of the symmetry-based

* Corresponding author. Fax: +44-23-8059-3781.
E-mail address: mhl@soton.ac.uk (M.H. Levitt).

0009-2614/$ - see front matter © 2004 Elsevier B.V. All rights reserved.
doi:10.1016/j.cplett.2004.03.075

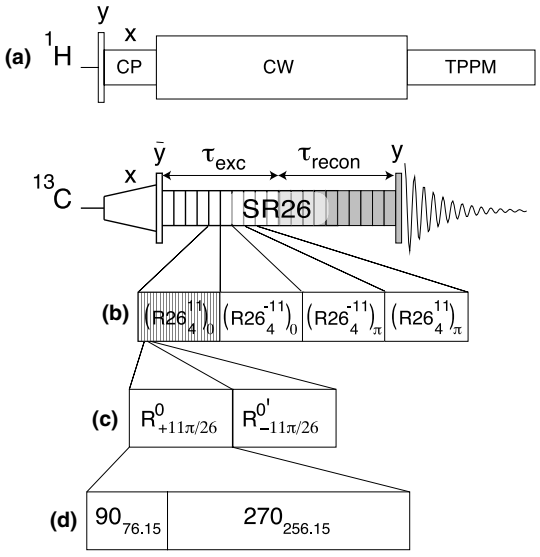

Fig. 1. (a) Pulse sequence used for double-quantum-filtered ^{13}C spectroscopy in organic solids, using the *SR*26 recoupling sequence. After cross-polarization, a 90° pulse is applied to the ^{13}C nuclei, to generate longitudinal magnetization. An *SR*26 sequence of duration τ_{exc} excites double-quantum coherence, which is reconverted into longitudinal magnetization by a second *SR*26 sequence, of duration τ_{recon}. In the constant-time procedure, the τ_{exc} is incremented and τ_{recon} is decremented so that the total interval $T = \tau_{exc} + \tau_{recon}$ is kept fixed. The shaded elements are given a four-step phase cycle. (b) Each *SR*26 supercycle contains two $R26_4^{11}$ and two $R26_4^{-11}$ recoupling cycles, with overall phase 0 or π. (c) Each $R26_4^{11}$ sequence consists of 13 *R*-element pairs. (d) Each *R*-element consists of two radiofrequency pulses.

recoupling sequences with the greater robustness of non-γ-encoded sequences. We describe a new pulse sequence of the form

$$SR26 = [R26_4^{11} R26_4^{-11}]_0 [R26_4^{-11} R26_4^{11}]_\pi, \tag{1}$$

where the symbol RN_n^v describes a symmetry-based pulse sequence given by:

$$RN_n^v = [(R^0)_{+\pi v/N} (R^0)'_{-\pi v/N}]^{N/2}, \tag{2}$$

where R^0 is a composite π pulse that rotates the resonant spin by $\pm\pi$ about the *x*-axis and $R^{0\prime}$ is derived from R^0 by changing the sign of all phases. The subscript determines the overall rf phase shifts of the *R*-elements, and the superscript determines the number of repetitions of the bracketed elements. The rf field is set so that one RN_n^v sequence occupies exactly *n* rotational periods of the sample. In the present case, the $R26_4^{11}$ sequences are based on the element $R^0 = R^{0\prime} = (\pi/2)_0(3\pi/2)_\pi$, leading to the explicit 208-pulse sequence:

$$\begin{aligned}&[90_{76.15}270_{256.15}90_{283.85}270_{103.85}]^{13}[90_{283.85}270_{103.85}90_{76.15}270_{256.15}]^{13}\\ &\quad\times|[90_{103.85}270_{283.85}90_{256.15}270_{76.15}]^{13}\\ &\quad\times[90_{256.15}270_{76.15}90_{103.85}270_{283.85}]^{13},\end{aligned} \tag{3}$$

where the phases and flip angles are given in degrees. The superscript denotes 13 repetitions of the bracketed elements, and the sequence spans 16 rotor periods. The hierarchical structure of this pulse sequence is shown in the timing diagram of Fig. 1.

The implementation of Eq. (3) requires a nutation frequency of 6.5 times the spinning frequency. We incorporate the pulse sequence of Eq. (3) in a constant-interval acquisition strategy as suggested by Tycko [21] and Schmedt auf der Günne [20]. We demonstrate that the *SR*26 sequence can be used for determining relatively long homonuclear distances with high DQ yields, even in systems with reasonably large CSA interactions. We demonstrate by simulation that the sequence has better performance than known competitors such as DRAWS.

2. Theory

2.1. Symmetry-based recoupling sequences

The theory of symmetry-based recoupling has been dealt with elsewhere [11–18], and only a brief summary will be given here. The interactions between the nuclear spins, the molecular environment and the external field can be classified in terms of their rotational properties [22], described by the integers l, m, λ, μ, where l and λ are the ranks with respect to spatial and spin rotations, respectively, and m and μ are the spatial and spin rotational quantum numbers. The spin evolution in the present of rf pulses can in many cases be described by average Hamiltonian theory [23]. In case of rotor-synchronized RN_n^v sequences, the average Hamiltonian terms obey the following selection rules [16]:

$$\overline{H}^{(1)}_{lm\lambda\mu} = 0 \quad \text{if } mn - \mu v \neq \frac{NZ_\lambda}{2}, \tag{4}$$

and

$$\overline{H}^{(2)}_{l_2 m_2 \lambda_2 \mu_2,\, l_1 m_1 \lambda_1 \mu_1} = 0 \quad \text{if} \begin{cases} m_1 n - \mu_1 v \neq \frac{N}{2} Z_{\lambda_1} \wedge \\ m_2 n - \mu_2 v \neq \frac{N}{2} Z_{\lambda_2} \wedge \\ (m_1 + m_2) n - (\mu_1 + \mu_2) v \neq \frac{N}{2} Z_{\lambda_1 + \lambda_2}. \end{cases} \tag{5}$$

The variable Z_λ is an even integer (including zero) when λ is even and is an odd number when λ is odd. Many homonuclear recoupling sequences have been designed using these selection rules [14,15,19]. In this Letter, we consider the sequence $R26_4^{11}$, for which the symmetry allowed terms in the first-order average Hamiltonian are $(l, m, \lambda, \mu) = (2, -1, 2, 2)$, $(2, 1, 2, -2)$ and (0,0,0,0), indicating a γ-encoded homonuclear double-quantum recoupling sequence. For the case of a homonuclear spin

pair with negligible J coupling the first-order average Hamiltonian is given by:

$$\overline{H}^{(1)}(R26_4^{11}) = \kappa\omega_{2-1}^{jk}\frac{1}{2}I_J^+I_k^+ + \kappa^*\omega_{21}^{jk}\frac{1}{2}I_J^-I_k^-, \quad (6)$$

where

$$\omega_{lm}^{jk} = [A_{lm}^{jk}]^R d_{m0}^l(\beta_{RL})\exp\{-\mathrm{i}m\alpha_{RL}^0\}. \quad (7)$$

Here $[A_{lm}^{jk}]^R$ is a space component of the dipole–dipole interaction tensor, written in the rotor-fixed frame, and α_{RL}^0 denotes the initial rotor phase. $[A_{lm}^{jk}]^R$ is obtained in the rotor-fixed frame by transforming it from the principal axis system in the usual way [22].

The scaling factor is $|\kappa| = 0.171$ for $R26_4^{11}$ with the basic element $R^0 = (\pi/2)_0(3\pi/2)_\pi$. This scaling factor is very similar to the scaling factor of $R14_2^6$ which is 0.172 [14]. However, the number of damaging second-order terms is much lower for $R26_4^{11}$ compared to $R14_2^6$ [14]. For example, the second-order selection rule Eq. (5) indicates that $R26_4^{11}$ has eight symmetry-allowed second-order terms involving commutators of two CSA × CSA Hamiltonians, while $R14_2^6$ has 20 terms of this form. Although the number of second-order terms is only a rough guide to sequence performance, we expect sequences such as $R26_4^{11}$ to be more robust than sequences of the symmetry $R14_2^6$.

2.2. Supercycles

Supercycling is applied to remove second and higher-order terms that are generated by the basic sequence $R26_4^{11}$. In the case of large chemical shift anisotropies the most damaging higher-order terms have the quantum numbers $\lambda_1 = \lambda_2 = 1$ and $\mu_1 = -\mu_2$. These terms generate an effective Hamiltonian component which is proportional to the z-angular momentum operator of the involved spins. The simulations of Karlsson et al. [9] show the destructive effect of these terms. By applying a supercycle of the form $[R26_4^{11}\,R26_4^{-11}]$ these terms may be destroyed in both the first and second-order average Hamiltonian, as shown by Brinkmann et al. [18]. The remaining CSA × CSA terms may be removed from the average Hamiltonian by an additional supercycle involving a π phase shift. The order of the cycles is changed in the second half of the sequence. This reduces the interference from higher-order terms even more. The theory of these supercycles will be published elsewhere. The full sequence in Eq. (3) is expected to be highly robust with respect to CSA interference and other imperfections. However, this benefit is achieved at the cost of the γ-encoding of the recoupled dipolar terms. The first-order average Hamiltonian for the supercycle is given by:

$$\overline{H}^{(1)}(SR26) = \mathrm{Re}(\kappa\omega^{jk*})\frac{1}{2}(I_j^+I_k^+ + I_j^-I_k^-). \quad (8)$$

The loss of γ-encoding results in a reduction in the dynamic range of the dipolar oscillations and leads to a loss in the maximum theoretical double-quantum filtering efficiency. However, these drawbacks are more than compensated at long recoupling times by the increased robustness of this sequence.

2.3. Constant-time acquisition

When recoupling sequences are used for relative long times, damping of the spin coherences plays a large role in the trajectory of the experimental observable. Damping may be caused by incoherent processes or by dissipation of the spin-order into multiple-spin coherences, for example through contact with abundant ^{1}H nuclei. It has been shown by Tycko and coworkers [21] and Schmedt auf der Günne [20] that the effects of relaxation or damping on the dipolar coupling estimate may be minimized by a so-called constant-time procedure. An appropriate pulse sequence for the double-quantum ^{13}C NMR of organic solids is sketched in Fig. 1. The shaded pulse-sequence elements are subject to a standard four-step phase-cycling procedure in order to select signals passing through ^{13}C double-quantum coherence, which must originate from coupled ^{13}C spin pairs. In the constant-time procedure the excitation interval τ_{exc} is increased in a series of experiments, while the double-quantum reconversion time τ_{recon} is decreased, so as to keep the total recoupling time $T = \tau_{\mathrm{exc}} + \tau_{\mathrm{recon}}$ constant. The result is an approximately symmetric curve with a maximum at $\tau_{\mathrm{exc}} = \tau_{\mathrm{recon}} = T/2$, which may be analyzed to obtain the homonuclear dipole–dipole coupling, with only minimal assumptions about relaxation. The drawback of this method is that a relatively long total recoupling time must be used to detect the dipolar oscillations.

3. Results

3.1. Simulations

Fig. 2 shows a set of simulations for a constant-time double-quantum-filtered experiment, using parameters appropriate to the $^{13}C_2$ system of [15,20-$^{13}C_2$]-all-E-retinal, at a magnetic field $B^0 = 9.4$ T. All simulations were performed using the SIMPSON program [24], with sets of 2003 molecular orientations generated by the Zaremba–Conroy–Cheng (ZCW) method [25]. The nutation frequency was 45.5 kHz, and the spinning frequency was 7 kHz. The spin-system parameters used in the simulation are given in Table 1. The X-ray diffraction estimate of the ^{13}C–^{13}C distance is 301.8 pm [26]. A constant recoupling time $T = 16$ ms was used to ensure good DQ-filtered efficiency and to maximize the

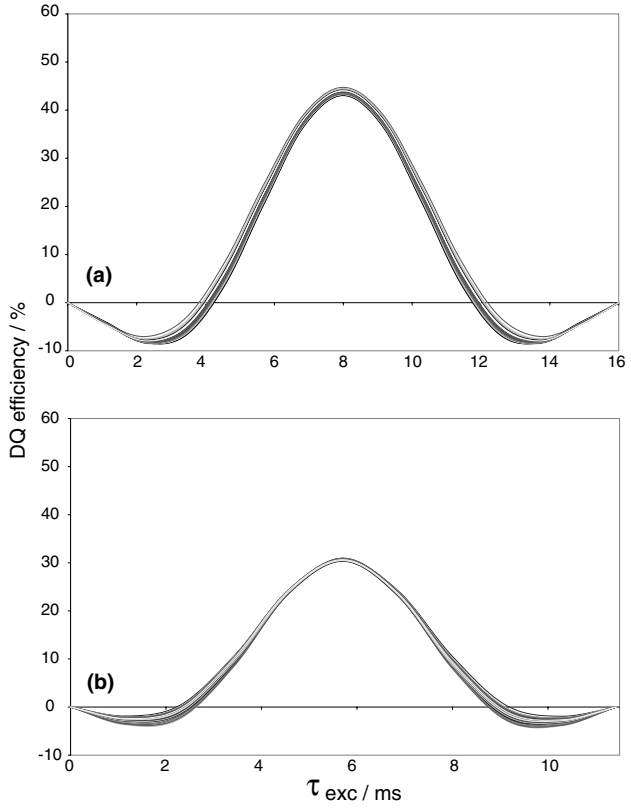

Fig. 2. Simulated DQ-filtered signal trajectories, using the parameters appropriate to [15,20 $^{13}C_2$]-all-E-retinal given in Table 1, at a spinning frequency of 7 kHz, and a field of 9.4 T: (a) simulation for *SR*26, changing the intervals τ_{exc} and τ_{recon} in steps of one-half of the full *SR*26 supercycle. A rf nutation frequency of 45.5 kHz was used; (b) simulation for DQ-DRAWS, using a rf nutation frequency of 59.5 kHz.

oscillations around the zero crossings. A DQ filtering efficiency of 43% is observed in simulations at $\tau_{exe} = \tau_{recon} = 8.00$ ms.

Fig. 2a shows a set of simulations corresponding to an ensemble of over 50 randomly chosen orientations of the CSA tensors and a 3% Gaussian distribution in the rf field amplitude. The rf field distribution reflects typical experimental conditions, while the randomized CSA orientations reflects the lack of detailed knowledge of the principal axis orientations in this case. It is clear from the simulation that the orientations of the CSA tensors and the rf field errors have little effect on the trajectory of the DQ-filtered signal. Other simulations showed that the rf field deviations are the main contribution to the spread in the observed curves.

Fig. 2b show similar results for the double-quantum DRAWS technique [7] using the version shown in Fig. 2a of the paper by Karlsson et al. [9] for comparison. The external field and rotation frequency was as in experiment (a). However, the rf nutation frequency was adjusted to 59.5 kHz (DRAWS requires a nutation frequency of 8.5 times the spinning frequency). A constant recoupling time $T = 11.42$ ms was used to maximize the double-quantum DRAWS signal. Despite the strong rf field, the overall simulated efficiency is much lower than for *SR*26. This behavior is typical for a wide range of simulated spin-systems.

3.2. Experiments

Fig. 3a,b shows experimental results obtained on diammonium [1,4-$^{13}C_2$]-fumarate, diluted to a level of 5.9% by cocrystallization with natural abundance material. This sample is referred to below as $^{13}C_2$–DAF. The ^{13}C–^{13}C distance is 387.8 pm [30], making it a challenging case for double-quantum filtering. The spectrum from an ordinary cross-polarization (CP) experiment is shown in Fig. 3a, while a double-quantum-

Table 1
Spin interaction parameters used in the NMR simulations, and internuclear distances determined by NMR and crystallography

Interactions	Diammonium [1,4-$^{13}C_2$]-fumarate [27]	[15,20-$^{13}C_2$]-all-E-retinal [28,29]
$\delta_j^{iso} - \delta_k^{iso}$ [a]	0	−176.3
δ_j^{aniso} [b]	−64.8	15.5
η_j^{aniso} [b]	0.82	1.0
$(\alpha_j, \beta_j, \gamma_j)$ [c]	(16,97,−103)	Unknown
$(\Delta\alpha_j, \Delta\beta_j, \Delta\gamma_j)$ [d]	(20,0,20)	iso
δ_k^{aniso} [b]	−64.8	−92.5
η_k^{aniso} [b]	0.82	0.51
$\alpha_k, \beta_k, \gamma_k$ [c]	(16,97,−103)	Unknown
$(\Delta\alpha_k, \Delta\beta_k, \Delta\gamma_k)$ [d]	(20,0,20)	iso
$(b_{jk}/2\pi)$/Hz [e]	-136.5 ± 5.1	-282.0 ± 4.9
r_{jk}/pm [f]	382.5 ± 4.5	299.8 ± 1.8
r_{jk}/pm [g]	387.8 [30]	301.8 [26]

[a] Isotropic shift difference between sites.
[b] CSA (deshielding units) and asymmetry parameter.
[c] Euler angles (°) relating the principal axis system of the CSA to the molecular reference frame.
[d] RMS deviation of Euler angles (°) used in the simulated ensemble. 'iso' indicates an isotropic distribution of CSA orientations.
[e] Measured dipole–dipole coupling.
[f] Estimated ^{13}C–^{13}C distance from the NMR measurements.
[g] ^{13}C–^{13}C distance from X-ray crystallography.

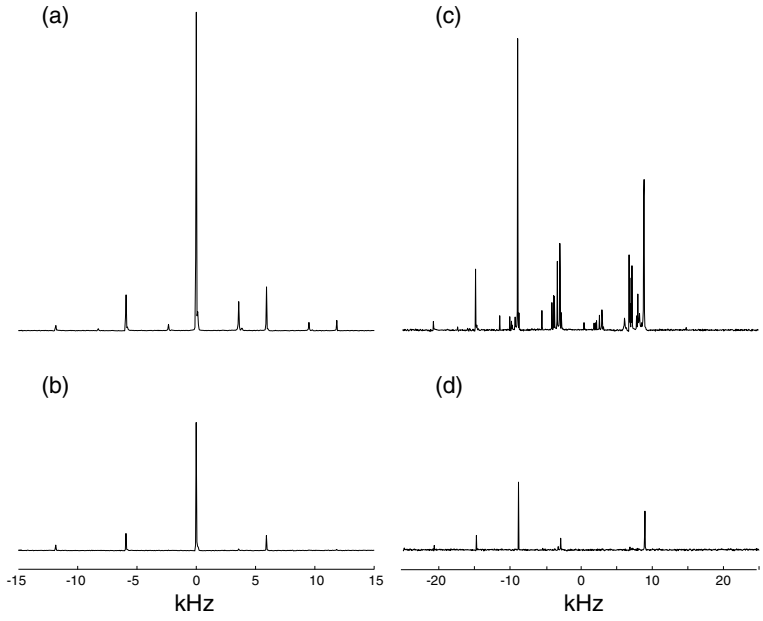

Fig. 3. (a) Cross-polarization ^{13}C spectrum of 5.9% diammonium [1,4-$^{13}C_2$]-fumarate. (b) DQ-filtered ^{13}C spectrum of 5.9% diammonium [1,4-$^{13}C_2$]-fumarate using a *SR*26 recoupling sequence, with $\tau_{exc} = \tau_{recon} = 10.8$ ms. (c) Cross-polarization ^{13}C spectrum of 10% [15,20-$^{13}C_2$]-all-E-retinal. (d) DQ-filtered ^{13}C spectrum of 10% [15,20-$^{13}C_2$]-all-E-retinal using a *SR*26 recoupling sequence, with $\tau_{exc} = \tau_{recon} = 5.4$ ms. See text for further details.

filtered spectrum is shown in Fig. 3b. These experiments were performed in a field of 9.4 T, spinning at 5.923 kHz, using a ^{13}C rf field providing a nutation frequency of 38.5 kHz, and a proton decoupler field corresponding to a nutation frequency of 100 kHz during the *SR*26 sequence. The signal acquisition was conducted using a decoupler field strength corresponding to a 84 kHz proton nutation frequency. TPPM modulation of the decoupler field was used to enhance the acquired NMR signals [31]. Fig. 3b illustrates the excellent 38.4% DQ efficiency obtained with the *SR*26 sequence, which is far larger than the 17% efficiency obtained in previous experiments using the $R22_4^9$ sequence [15]. This high efficiency confirms that the theoretical loss of efficiency associated with the lack of γ-encoding is compensated by the greater robustness of the supercycle at long times.

Fig. 3c,d shows experimental results for [15,20-$^{13}C_2$]-all-E-retinal diluted to 10% by recrystallization with unlabeled all-E-retinal. In Fig. 3c the CP spectrum is shown while the DQ-filtered spectrum is shown in Fig. 3d. As may be seen, DQ-filtering suppresses the many natural abundance ^{13}C peaks from the unlabeled retinal sites. In this case we obtained a maximum in the DQ efficiency of 18.8%, while simulations in the absence of relaxation showed a maximum of 51.5%. The loss of signal is attributed to imperfectly decoupled heteronuclear interactions during the *SR*26 sequence. In this case, the observed double-quantum efficiency of 18.8% is very similar to that achieved using a γ-encoded sequence [15]. These results confirm that heteronuclear interactions often provide the main obstacle to double-quantum recoupling at longer distances. Although the suppression of natural-abundance ^{13}C peaks is almost complete, small peaks from unlabeled ^{13}C sites are visible in both the double-quantum-filtered spectra of Fig. 3b,d. We believe that these residual peaks are due to double-quantum excitation of spin pairs comprising one labeled ^{13}C site and one ^{13}C nucleus in natural abundance. These peaks disappeared at short double-quantum recoupling times. Fig. 4a shows experimental double-quantum-filtered signal amplitudes for [1,4-$^{13}C_2$]-fumarate, along with simulated curves. Neighboring experimental points correspond to an incrementation of τ_{exc} by one-half of a supercycle, and decrementation of τ_{recon} by the same amount. The figure show a good fit between simulations and experiment for a ^{13}C–^{13}C dipolar coupling of −133 Hz. The only fit parameter in the simulation was the overall vertical scale. Two other curves at −128 and −138 Hz are also shown. The slight decrease in the DQ yield as compared to the maximum shown in Fig. 3 is due to the longer total evolution time T which is needed in order to define the dipolar oscillations properly. The simulated curves in Fig. 4a,b shows that the zero crossings are particularly sensitive to the magnitude of the dipolar coupling. The accuracy of the measured dipolar coupling therefore depends strongly on an accurate determination of the experimental points near the zero crossings and their confidence limits. In order to estimate the rigorous confidence limits on the dipolar coupling estimate, an ensemble of spin-system parameters was generated, with a distribution of rf fields and randomized CSA

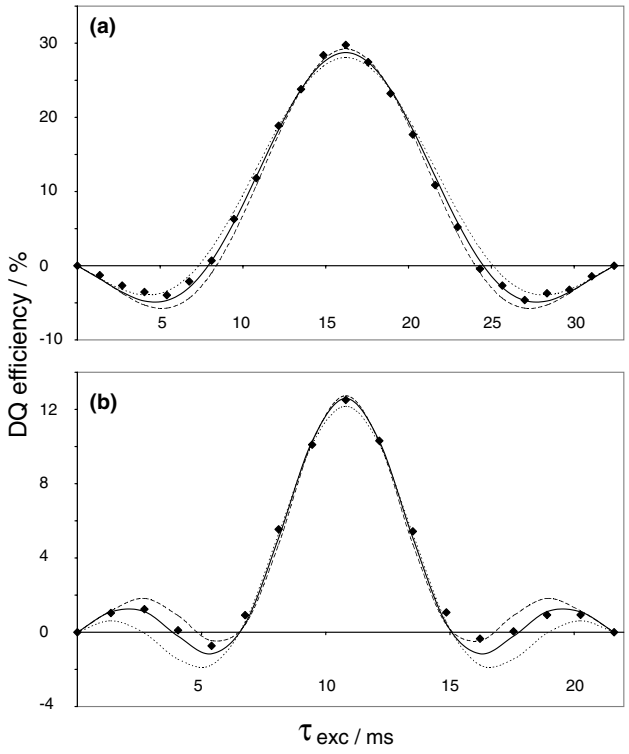

Fig. 4. (a) Double-quantum-filtered signal amplitudes for 5.9% diammonium [1,4-$^{13}C_2$]-fumarate, plotted against the excitation interval τ_{exc}, using a constant total recoupling interval $T = 32.42$ ms. The diamonds are the experimental points. The solid line is the best fit simulation corresponding to the dipole–dipole −133 Hz, with dashed lines corresponding to deviations of ±5 Hz. (b) Double-quantum-filtered signal amplitudes for 10% [15,20-$^{13}C_2$]-all-E-retinal, using a constant total recoupling interval $T = 21.61$ ms. The diamonds are the experimental points. The solid line is the best fit simulation corresponding to the dipole–dipole constant −282 Hz, with dashed lines corresponding to deviations of ±20 Hz. Experimental details as in Fig. 3.

orientations as used in Fig. 2. For each ensemble member, the dipolar coupling and the overall vertical scale factor was optimized to produce the best fit between experiment and simulation, using the SIMPSON Minuit routine [32]. This procedure generated a set of dipolar coupling values which was analyzed statistically to provide a dipolar coupling estimate and confidence limits, as summarized in Table 1. There is good agreement between the ^{13}C–^{13}C distances determined by X-ray crystallography (387.8 pm) and double-quantum NMR (382 ± 4 pm). The residual difference of about 6 ± 4 pm (0.05 Å) may be partly due to the different influence of vibrational motion in the two experimental techniques.

4. Conclusions

The *SR*26 sequence has been shown by simulations and experiments to be highly robust with respect to CSA interactions and rf field errors. The sequences appears to be particularly suitable for the measurement of small homonuclear couplings without detailed knowledge of the CSA orientations. In the case of relative long ^{13}C–^{13}C distances, the supercycled $R26_4^{11}$ sequence gives higher DQ yields and is less dependent on correct knowledge of the CSA orientations than previous techniques. The good experimental performance of this pulse sequence, with a double-quantum filtering efficiency of 38% in a sample with an internuclear distance of nearly 400 pm is very promising for future applications.

Acknowledgements

This research was supported by the ERSRC (UK) and the NSF (Norway). We thank J. Schmedt auf der Günne for making a manuscript available prior to publication. We thanks H. Luthman for synthesis of the [15,20-$^{13}C_2$]-all-E-retinal, and A. Sebald for providing us with the diammonium [1,4-$^{13}C_2$]-fumarate.

References

[1] F. Castellani, B. van Rossum, A. Diehl, M. Schubert, K. Rehbein, H. Oschkinat, Nature 420 (2002) 98.
[2] D.P. Raleigh, M.H. Levitt, R.G. Griffin, Chem. Phys. Lett. 146 (1988) 71.
[3] T. Gullion, J. Schaefer, J. Magn. Reson. 81 (1989) 196.
[4] R. Tycko, G. Dabbagh, Chem. Phys. Lett. 173 (1990) 461.
[5] D.M. Gregory, D.J. Mitchell, J.A. Stringer, S. Kiihne, J.C. Shiels, J. Callahan, M.A. Mehta, G.P. Drobny, Chem. Phys. Lett. 246 (1995) 654.
[6] M.A. Mehta, D.M. Gregory, S. Kiihne, D.J. Mitchell, M.E. Hatcher, J.C. Shiels, Solid State Nucl. Magn. Res. 7 (1996) 211.
[7] D.M. Gregory, G.M. Wolfe, T.P. Jarvie, J.C. Shiels, G.P. Drobny, Mol. Phys. 89 (1996) 1835.
[8] D.M. Gregory, M.A. Mehta, J.C. Shiels, G.P. Drobny, J. Chem. Phys. 107 (1997) 28.
[9] T. Karlsson, J.M. Popham, J.R. Long, N. Oyler, G.P. Drobny, J. Am. Chem. Soc. 125 (2003) 7394.
[10] N.C. Nielsen, H. Bildsøe, H.J. Jakobsen, M.H. Levitt, J. Chem. Phys. 101 (1994) 1805.
[11] Y.K. Lee, N.D. Kurur, M. Helmle, O.G. Johannessen, N.C. Nielsen, M.H. Levitt, Chem. Phys. Lett. 242 (1995) 304.
[12] M. Hohwy, H.J. Jakobsen, M. Edén, M.H. Levitt, N.C. Nielsen, J. Chem. Phys. 108 (1998) 2686.
[13] A. Brinkmann, M. Edén, M.H. Levitt, J. Chem. Phys. 112 (2000) 8539.
[14] M. Carravetta, M. Edén, A. Brinkmann, X. Zhao, M.H. Levitt, Chem. Phys. Lett. 321 (2000) 205.
[15] M. Carravetta, M. Edén, O.G. Johannessen, H. Luthman, P.J.E. Verdegem, J. Lugtenburg, A. Sebald, M.H. Levitt, J. Am. Chem. Soc. 123 (2001) 10628.
[16] A. Brinkmann, M.H. Levitt, J. Chem. Phys. 115 (2001) 357.
[17] M.H. Levitt, Encyclopedia of Nuclear Magnetic Resonance: Supplementary Volume, 2002, p. 165.
[18] A. Brinkmann, J. Schmedt auf der Günne, M.H. Levitt, J. Magn. Reson. 156 (2002) 79.
[19] P.E. Kristiansen, D.J. Mitchell, J.N.S. Evans, J. Magn. Reson. 157 (2002) 253.

[20] J. Schmedt auf der Günne, J. Magn. Reson. 165 (2003) 18.
[21] A.E. Bennett, D.P. Weliky, R. Tycko, J. Am. Chem. Soc. 120 (1998) 4897.
[22] M. Mehring, Principles of High Resolution NMR in Solids, Springer, Berlin, 1983.
[23] U. Haeberlen, J.S. Waugh, Phys. Rev. 175 (1968) 453.
[24] M. Bak, J.T. Rasmussen, N.C. Nielsen, J. Magn. Reson. 147 (2000) 296.
[25] H. Conroy, J. Chem. Phys. 47 (1967) 5307.
[26] T. Hamanaka, T. Mitsui, T. Ashida, M. Kakudo, Acta Cryst. B 28 (1972) 214.
[27] M. Bechmann, X. Helluy, A. Sebald, J. Magn. Reson. 152 (2001) 14.
[28] P.J.E. Verdegem, M. Helmle, J. Lugtenburg, H.J.M. de Groot, J. Am. Chem. Soc. 119 (1997) 169.
[29] G.S. Harbison, P.P. Mulder, H. Pardoen, J. Lugtenburg, J. Herzfeld, R.G. Griffin, J. Am. Chem. Soc. 107 (1985) 4809.
[30] H. Hosomi, Y. Ito, S. Ohba, Acta Cryst. C 54 (1998) 142.
[31] A.E. Bennett, C.M. Rienstra, M. Auger, K.V. Lakshmi, R.G. Griffin, J. Chem. Phys. 103 (1998) 6951.
[32] T. Vosegaard, A. Malmendal, N.C. Nielsen, Chem. Monthly 133 (2002) 1555.